Moisture Sorption Kinetics for Water-Soluble Substances III: Theoretical and Experimental Studies in Air

L. VAN CAMPEN *, G. L. AMIDON ‡, and G. ZOGRAFI ˣ

Received June 9, 1982, from the *School of Pharmacy, University of Wisconsin-Madison, Madison, WI 53706.* Accepted for publication October 22, 1982. Present addresses: *Boehringer Ingelheim Ltd., Ridgefield, CT 06877 and ‡College of Pharmacy, University of Michigan, Ann Arbor, MI 48104.

Abstract □ As an extension of the model of heat transport control developed for the kinetics of water sorption by water-soluble substances from an atmosphere of pure water vapor, equations have been developed to account for limitations of diffusion on mass transport of water vapor when air is present. Although the inability to determine the vapor diffusion layer thickness prevents using these equations to predict sorption behavior *a priori*, minimum water sorption rates can be calculated by assuming a diffusion layer thickness equal to the sample chamber radius. Combining heat transport and mass transport produces equations which describe very well the observed sorption by three water-soluble salts in one atmosphere of air. As in the absence of air, sorption rates are predicted and observed to be constant at a given atmospheric relative humidity.

Keyphrases □ Sorption—moisture, water-soluble substances, kinetics, theoretical model with air atmosphere, application to potassium bromide, potassium iodide, and choline iodide □ Kinetics—moisture sorption by water-soluble substances, theoretical model with air atmosphere, application to potassium bromide, potassium iodide, and choline iodide □ Deliquescence—kinetics of water sorption, theoretical model with air atmosphere, application to potassium bromide, potassium iodide, and choline iodide

In the first paper in this series (1) a theoretical model for the kinetics of water sorption by water-soluble solids exhibiting deliquescence was developed based on a heat transport control model. This model was tested successfully for water sorption from an atmosphere of pure water vapor over wide ranges of relative humidity in the second paper (2). In the present paper, this work is extended to include water sorption kinetics from an atmosphere containing air at approximately 1 atm of pressure. In such a case, one would expect the effects of diffusion through air on the mass transport of water vapor to influence the overall process. A model for water sorption in air is developed herein, first by assuming that only mass transport occurs and then by combining this with the heat transport model previously developed (1). Within the constraints of applying a mass transport model *a priori*, several water sorption experiments in an atmosphere of air have been performed to illustrate the potential importance of mass and heat transport in such a process.

THEORETICAL

Mass Transport Model (Isothermal)—As described in detail in the first paper (1) the thermodynamic basis for water uptake by water-soluble solids lies in the difference between equilibrium water vapor pressure, P_s, over the saturated solution of the solid and that in the atmosphere surrounding the solid, P_c. As seen in Fig. 1, when the heat sinks surrounding the liquid–vapor interface are sufficient in efficiency and capacity so as to maintain the system isothermal at T_c ($\Delta T = 0$), the rate of steady-state uptake is directly proportional to the constant water vapor pressure difference, $\Delta P = P_c - P_s$, over the vapor diffusion layer adjacent to the liquid–vapor interface. Expressed in terms of relative humidity, this difference becomes:

$$(100)\frac{\Delta P}{P_0} = RH_i - RH_o \qquad \text{(Eq. 1)}$$

where RH_i is the independent variable in a moisture-uptake experiment.

The radial diffusive flux of water vapor through a nondiffusing gas can be described by the following expression:

$$W'_{sp} = x_w W'_{sp} - M_w c D \frac{dx_w}{dr} \qquad \text{(Eq. 2)}$$

where W'_{sp} is the mass of water vapor transported in the z-direction per unit time per unit area, x_w is the mole fraction of water vapor in the atmosphere, M_w is the molecular weight of water, c is the total molar concentration in the atmosphere, and D is the binary diffusion coefficient of water vapor in the atmosphere. The first term in the right-hand side of Eq. 2 pertains to the mass flux of water vapor resulting from bulk fluid motion (where that of the inert gas is considered negligble) and the second term results from the diffusive mass flux of vapor superimposed on the bulk flow. Solving for W'_{sp} and expressing x_w in terms of pressure P, assuming gas ideality such that:

$$x_w = P/(P + P_i) \qquad \text{(Eq. 3)}$$

where P_i is inert gas pressure, one obtains:

$$W'_{sp} = -\frac{M_w c D}{P_T - P}\frac{dP}{dr} \qquad \text{(Eq. 4)}$$

where P_T represents the total (water vapor and inert gas) pressure. Here it is assumed that the temperature dependence of relative humidity is independent of the partial pressure of any inert gas present (3), and that the diffusion coefficient is independent of water vapor concentration and temperature.

Steady-state radial diffusion requires that:

$$\frac{d}{dr}(r^2 W'_{sp}) = 0 \qquad \text{(Eq. 5)}$$

Substitution of the expression for mass flux, W'_{sp}, from Eq. 4 then gives:

$$\frac{d}{dr}\left(r^2 \frac{M_w c D}{P_T - P}\frac{dP}{dr}\right) = 0 \qquad \text{(Eq. 6)}$$

When this expression is integrated over the boundary conditions for a hollow sphere[1], given as $P = P_s$ at $r = a$ and $P = P_c$ at $r = a'$, where $a' - a = \delta$ = effective thickness of the vapor diffusion layer, the following

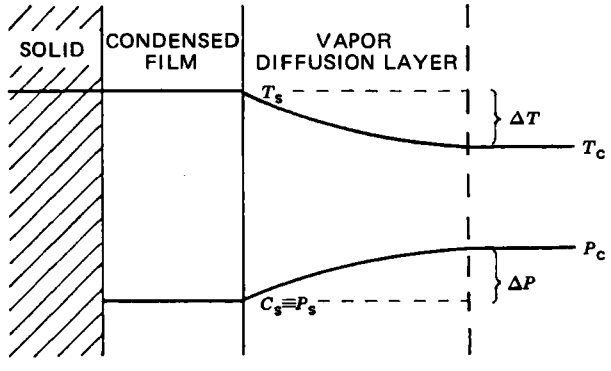

Figure 1—*Thermal and pressure gradients existing at a soluble solid surface covered with condensed water.*

[1] A hollow-sphere geometry was chosen earlier (1) for the development of the heat transport control model, and hence, it will also be carried through in this series of derivations.

0022-3549/83/1200-1394$01.00/0

relation is obtained:

$$\ln (P_T - P) = \left(\frac{\frac{1}{r} - \frac{1}{a}}{\frac{1}{a'} - \frac{1}{a}}\right) \ln \left(\frac{P_T - P_c}{P_T - P_s}\right) + \ln (P_T - P_s) \quad \text{(Eq. 7)}$$

From Eq. 4, the mass flux at surface $r = a$ is given as:

$$W'_{sp}\Big|_{r=a} = M_w c D \left.\frac{d \ln (P_T - P)}{dr}\right|_{r=a} \quad \text{(Eq. 8)}$$

for which the derivative is evaluated on the basis of Eq. 7 to yield:

$$W'_{sp}\Big|_{r=a} = -M_w c D \left(\frac{1}{\frac{a^2}{a'} - a}\right) \ln \left(\frac{P_T - P_c}{P_T - P_s}\right) \quad \text{(Eq. 9)}$$

Since mass is conserved, the mass flux across any spherical surface in the system is:

$$W' = 4\pi a^2 W'_{sp}\Big|_{r=a} \quad \text{(Eq. 10)}$$

$$= \left(\frac{4\pi M_w c D}{\frac{1}{a} - \frac{1}{a'}}\right) \ln \left(\frac{P_T - P_c}{P_T - P_s}\right) \quad \text{(Eq. 11)}$$

or, rearranged and expressed in terms of relative humidity:

$$W' = W'_m = -\left(\frac{60 \cdot 4\pi M_w c D}{\frac{1}{a} - \frac{1}{a'}}\right) \ln \left(\frac{100(P_T/P_0) - RH_o}{100(P_T/P_0) - RH_i}\right) \quad \text{(Eq. 12)}$$

where a factor of 60 has been included to convert W' (or W'_m to indicate mass transport control) to units of mg/min, given that M_w has units of mg/mole, c has units of mole/cm^3, and D has units of cm^2/sec. This equation is then the solution for steady-state radial mass diffusion in a hollow sphere. The negative sign for W' in Eq. 12 when $RH_o < RH_i$ reflects water vapor diffusion in the negative r-direction, consistent with the condensation process.

In the case where $P \ll P_T$, integration of Eq. 4 over the same boundary conditions followed by the evaluation of dP/dr at $r = a$ in the same manner given above, leads to the analogous expression for W'_m:

$$W'_m = -\frac{60 \cdot 4\pi M_w c D P_0}{100 P_T \left(\frac{1}{a} - \frac{1}{a'}\right)} (RH_i - RH_o) \quad \text{(Eq. 13)}$$

In addressing the question of the time required to reach steady state, the solution for the time-dependent radial pressure gradient in the atmosphere is readily obtained from the non-steady-state mass transport equations developed in Appendix I of the first paper in this series (1). From this, the time required for the steady-state diffusion expressed by Eq. 13 to establish itself can be determined. In terms of dimensionless concentration, pressure, or relative humidity (at a given constant temperature), this solution comes directly from Eq. A8 in Appendix I of Ref. 1:

$$C^* = P^* = RH^* = \left[\frac{1}{r^*(a'/a - 1) + 1}\right] \times \left[1 - r^* - \frac{2}{\pi} \sum_{n=1}^{\infty} \frac{1}{n} \sin n\pi r^* \cdot \exp(-n^2\pi^2 t^*)\right] \quad \text{(Eq. 14)}$$

where C^*, P^*, and RH^* are all defined analogously with the definition of Π^*, and where:

$$t^* = \frac{Dt}{(a' - a)^2} \quad \text{(Eq. 15)}$$

and

$$r^* = \frac{r - a}{a' - a} \quad \text{(Eq. 16)}$$

This function is described in Fig. 6 of Ref. 1 where $\Pi^* = C^*$ and $a' = b$. Since the time to steady state increases as $a' \to b$, allowing $a' = b$ should result in a conservative estimate of the time required for the pressure gradient to establish itself. In 1 atm of air, the time then required to reach $t^* = 0.5$ is only 4.3 sec using the constants given in Table I. Thus, even at the likely maximum diffusion layer thickness of 2 cm, pressure gradients within the system should be rapidly established relative to the time scale of extended uptake.

Table I—Physical Constants for the Transport Model in 1 atm of Air

Symbols	Constants
a, cm	0.5[a]
b, cm	2.05
P_0, atm	3.12×10^{-4}
P_T, atm	1
M_w, mg/mole	1.8×10^4
D, cm^2/sec	0.258[b]
c, moles/cm^3	4.09×10^{-5}
k, cal/cm · sec · deg	6.22×10^{-5} [c]
α, cm^2/sec	0.214[d]
ΔH_v, cal/mole	10500
R, cal/deg · mole	1.987
T_c, °K	298
σ, cal/cm^2·sec·deg^4	1.36×10^{-12}
e	0.95[e]

[a] Characteristic disk thickness unique to each compound examined; range = 0.492–0.512 cm. [b] Calculated according to Ref. 5 for water vapor in the presence of a nonpolar inert gas. [c] Calculated using the Lindsay and Bromley modification of the Wassiljewa equation (6). [d] Used in calculations were C_p values weighted by mole fraction and k as indicated above. [e] Film surface emissivity approximated by value given for pure water (7).

The time required for the mass flux to reach a steady-state level can be calculated from the lag time at surface $r = a$ whose solution is given by the analogous form of Eq. A21 (*cf.* Ref. 1) for mass diffusion:

$$t_{lag,r=a} = -\frac{a(a' - a)^2}{3Da'} \quad \text{(Eq. 17)}$$

For the example above, this lag time equals (−)0.72 sec, where again the value of a' is taken to its extreme value of $b = 2$ cm. At surface $r = b$, a lag time of 1.4 sec is calculated using the analogous form of Eq. A25 (*cf.* Ref. 1) for $a' = b$:

$$t_{lag,r=b} = \frac{(b - a)^2}{6D} \quad \text{(Eq. 18)}$$

It is clear from these results that in the system containing air, the measurement of steady-state uptake rates should not be precluded by the transient effects associated with the establishment of the steady-state pressure gradient driving the uptake.

Combined Mass–Heat Transport Model—The uptake rate W' in air is explicitly dependent on the difference in relative humidity, $RH_i - RH_o$, as described by Eq. 13 when condensation is limited by water vapor diffusion to the sample. When the process is limited by heat transport, however, W' exhibits only an implicit dependence on this difference as given below in Eq. 19, developed earlier (1):

$$W'_h = \left[\frac{60 M_w \cdot 4\pi k a b}{\Delta H (b - a)} \left(\frac{R T_c^2}{\Delta H_v - R T_c \ln \frac{RH_i}{RH_o}}\right) + \frac{60 M_w \cdot 4\pi a^2 \sigma e}{\Delta H} \left(\frac{4 R T_c^5}{\Delta H_v - 4 R T_c \ln \frac{RH_i}{RH_o}}\right)\right] \cdot \ln \frac{RH_i}{RH_o} \quad \text{(Eq. 19)}$$

When heat and mass transport are in balance, these equations must be solved simultaneously, since in this case neither the humidity difference (now $< RH_i - RH_o$) which drives mass transport, nor ΔT (now $< \Delta T_{max}$ as estimated by the Clausius–Clapeyron relation in Eq. 20 below) which drives heat transport, can be predicted *a priori*. As before (1):

$$\Delta T_{max} = \frac{R T_c^2 \ln \frac{RH_i}{RH_o}}{\Delta H_v - R T_c \ln \frac{RH_i}{RH_o}} \quad \text{(Eq. 20)}$$

Scheme I illustrates the interrelationship between the effective difference in relative humidity, $\Delta RH = RH_i - RH_s$, where RH_s is the effective relative humidity (relative to P_0 at 25°) at the sample surface, and

the experimentally controlled $\Delta RH = RH_i - RH_o$. The Clausius–Clapeyron equation now relates RH_o to RH_s, where the analogous form of Eq. 20 becomes:

$$\begin{array}{ccccc} & \text{Clausius–Clapeyron Equation} & & & \\ P_s^{(T_c)} & \longrightarrow & P_s^{(T_s)} & < & P_c^{(T_c)} \\ \| & & \| & & \| \\ RH_o & < & RH_s & < & RH_i \end{array}$$

Scheme I

$$\Delta T = T_s - T_c = \frac{RT_c^2 \ln \frac{RH_s}{RH_o}}{\Delta H_v - RT_c \ln \frac{RH_s}{RH_o}} \quad \text{(Eq. 21)}$$

Accounting for Eq. 21 in deriving an equation for the dependence of W' on ΔT as in Eq. 19, one obtains:

$$W' = \left[\frac{60M_w \cdot 4\pi kab}{\Delta H(b-a)}\left(\frac{RT_c^2}{\Delta H_v - RT_c \ln \frac{RH_s}{RH_o}}\right) + \frac{60M_w \cdot 4\pi a^2 \sigma e}{\Delta H}\left(\frac{4RT_c^5}{\Delta H_v - 4RT_c \ln \frac{RH_s}{RH_o}}\right)\right] \cdot \ln \frac{RH_s}{RH_o} \quad \text{(Eq. 22)}$$

The analogous transformation for mass transport (when $P \ll P_T$) as given by Eq. 13 becomes:

$$W' = -\frac{60 \cdot 4\pi M_w c D P_0}{100 P_T \left(\frac{1}{a} - \frac{1}{a'}\right)}(RH_i - RH_s) \quad \text{(Eq. 23)}$$

$$= -k_m A(RH_i - RH_s) \quad \text{(Eq. 24)}$$

where k_m, is a mass transport coefficient for diffusive flux over area $A = 4\pi a^2$, is given by:

$$k_m = \frac{60M_w c D P_0}{100 P_T \left(a - \frac{a^2}{a'}\right)} \quad \text{(Eq. 25)}$$

Since neither T_s nor RH_s is known in Eqs. 21–23, however, the above expressions for W' are not useful in their present form. Furthermore, because of the complex logarithmic dependence of W' on RH_s in Eq. 22 and linear dependence in Eq. 23, RH_s cannot be eliminated analytically from their simultaneous solution. For predictive purposes, therefore, it becomes worthwhile to introduce two approximations.

The first useful approximation entails linearizing the relationship between temperature and relative humidity in Eq. 21. This can be accomplished by establishing an empirical relation based on P_0-values covering an experimentally appropriate range in T_s and T_c. Consider moisture sorption by common alkali halide salts: according to the above model, heat transport-controlled sorption is predicted to occur over a $\Delta T < 10°$ at $T_c = 298°K$. Assuming that the water vapor pressure over a salt solution has the same temperature dependence as that over pure water, the variation of P_0 between 298°K and 303°K on conversion to relative humidity yields the following predictive equation for RH_s as a function of T_s:

$$RH_s - RH_o = 0.0679 \cdot RH_o(T_s - T_c) \quad \text{(Eq. 26)}$$

For sodium chloride this relation overestimates the reported value for RH_s at $T_s = 302.4°K$ (4) by only 0.5%.

The second useful approximation addresses the dependence of the radiation term on $\Delta(T^4)$. Allowing:

$$T_s^4 - T_c^4 = 4T_c^3(T_s - T_c) \quad \text{(Eq. 27)}$$

where $T_c = 298°K$ and $T_s = 313°K$, this approximation underestimates the value of $\Delta(T^4)$ by <7.5% even at an extreme ΔT of 15°.

The combination of Eqs. 1 and 31 from Ref. 1 with Eq. 27 (above), *including the units* conversion factor of $60M_w$, leads to a simpler expression for the dependence of W' on ΔT:

$$W' = \left[\frac{60M_w \cdot 4\pi kab}{\Delta H(b-a)} + \frac{4T_c^3 \cdot 60M_w \cdot 4\pi a^2 \sigma e}{\Delta H}\right] \cdot \Delta T \quad \text{(Eq. 28)}$$

Substituting for ΔT from Eq. 26 gives:

$$W' = k_h A(RH_s - RH_o) \quad \text{(Eq. 29)}$$

where k_h is a heat transport coefficient for heat flux over the surface of area $A = 4\pi a^2$, and is given by:

$$k_h = -\frac{14.72}{RH_o}\left[\frac{60M_w kb}{a\Delta H(b-a)} + \frac{4T_c^3 \cdot 60M_w \sigma e}{\Delta H}\right] \quad \text{(Eq. 30)}$$

Solving for RH_s in Eq. 29 and substituting the result into Eq. 24, one obtains:

$$W' = -k_m A(RH_i - RH_o + W'/k_h A) \quad \text{(Eq. 31)}$$

On rearranging, a final equation for W' is obtained in which the effects of both heat and mass transport (for systems in which $P \ll P_T$) are accounted for:

$$W' = W'_{mh} = -\frac{k_m k_h}{k_m + k_h} A(RH_i - RH_o) \quad \text{(Eq. 32)}$$

or

$$W'_{mh} = -\frac{60M_w \cdot 4\pi c D P_0(RH_i - RH_o)}{100P_T\left(\frac{1}{a} - \frac{1}{a'}\right) - \frac{cDP_0 \cdot \Delta H(b-a)RH_o}{14.72[kab + 4T_c^3 a^2 \sigma e(b-a)]}} \quad \text{(Eq. 33)}$$

The contribution of the mass–heat transport coupling is reflected by the demoninator of this equation: as the second term vanishes, as for a system with $k = \infty$ where $\Delta T \to 0$, the mass transport control relation of Eq. 13 remains. Conversely, as the vapor diffusion layer becomes infinitesimal as $a' \to a$, Eq. 33 reduces to an expression similar in form to Eq. 28 wherein the logarithmic dependence of ΔT on RH_i has been effectively linearized.

EXPERIMENTAL

Materials—The sources and treatment of potassium iodide, potassium bromide, and choline iodide have been presented in the preceding paper (2).

Methods—The preparation of disks, the apparatus used, and the method of treating data were described in the preceding paper (2), with one important change instituted in the present study. The very slow diffusion of water vapor from the relative humidity chambers to the sample through an atmosphere of air precluded use of the chambers as described previously. Therefore, a small volume of saturated salt solution, containing an excess of salt, whose RH_o equalled the desired RH_i, was placed directly into the sample tube. The tube was capped and shaken for several minutes prior to use to accelerate humidity equilibrium. The chamber was then rapidly set in place around the loaded sample, with air thus present at a pressure of approximately 1 atm.

To assure that the value of RH_i in the chamber containing air was known and constant during a run, an electronic humidity sensor[2] was installed within the sample chamber. This consisted of a thin rectangular block of cross-linked polystyrene copolymer. The impedance changes caused by sorption and desorption of water were measured by an AC bridge circuit, capable of measuring a maximum value of 1.1 MΩ. Calibration was carried out by exposing the sensor, placed in the sample chamber at atmospheric air pressure, to known relative humidities. The temperature change, ΔT, near the sample surface was also monitored with a thermocouple, as previously described (2).

RESULTS

Since the diffusion layer thickness, δ, is unknown, neither Eq. 13 nor Eq. 33 can be used to predict *a priori* uptake rates for a given system. In the case where a' approaches the radius of the sample tube, b, and hence where $\delta = b - a$, the diffusional barrier would be maximized such that the rate of water sorption would be at a minimum value of W'. Using appropriate values of the various parameters needed to apply Eqs. 13 (for W'_m) and 33 (for W'_{mh}) found in Table I, and also using parameters in Table I needed to apply Eq. 19 for W'_h for the heat transport model in an atmosphere of air, three theoretical plots can be produced to describe

[2] Phys-Chemical Research Corp.

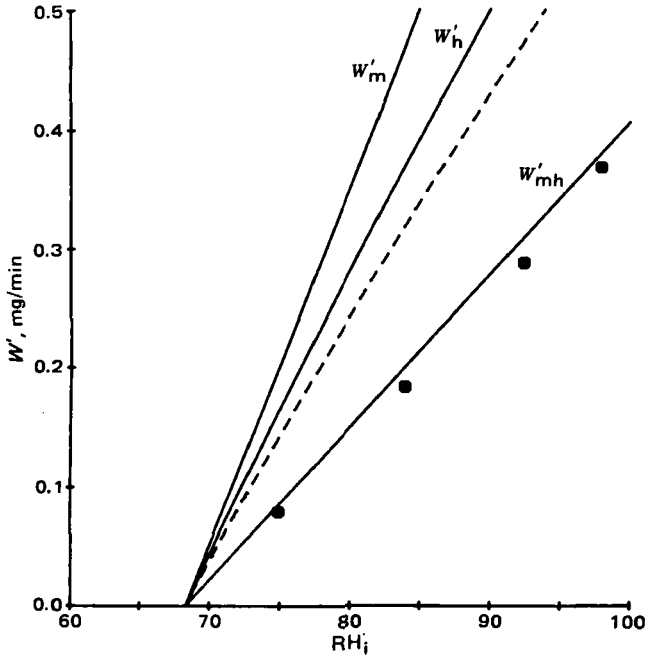

Figure 2—*Sorption rates in 1 atm air for disks of potassium iodide as a function of RH. The solid lines are theoretical sorption curves for* W'_m, W'_h *(air), and* W'_{mh} *plotted according to Eqs. 13, 19, and 33, respectively. The dashed line presents the corresponding theoretical curve for heat transport-controlled sorption in the absence of inert gas.*

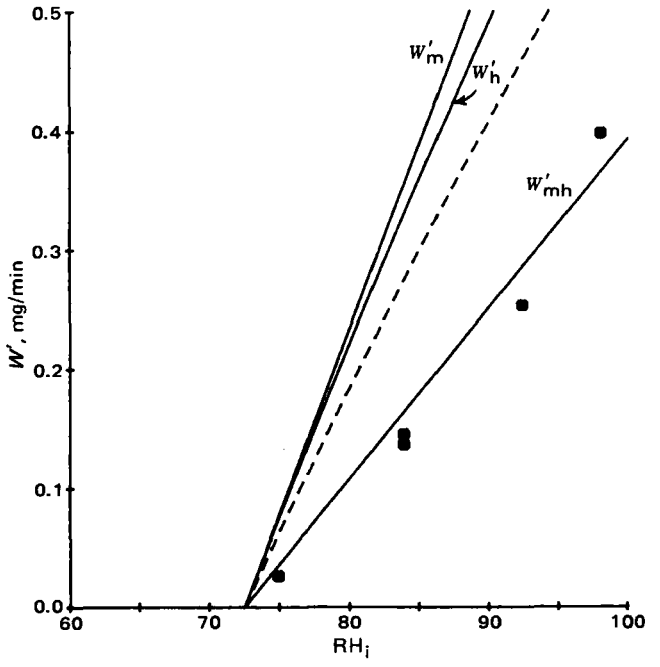

Figure 4—*Sorption rates in 1 atm of air for disks of choline iodide as a function of RH. The solid lines are theoretical sorption curves for* W'_m, W'_h *(air), and* W'_{mh} *plotted according to Eqs. 13, 19 and 33, respectively. The dashed line presents the corresponding theoretical curve for heat transport-controlled sorption in the absence of inert gas.*

water sorption rates as a function of RH_i. Figures 2–4 present comparisons of these theoretical curves with experimental results for potassium iodide, potassium bromide, and choline iodide, respectively. For the sake of further comparison, the corresponding theoretical plots as shown in the preceding paper (2) for water sorption in the absence of any inert gas, where heat transport strictly controls uptake, are also included in each case.

From the theoretical plots, it is clear that mass transport over a vapor diffusion layer of finite thickness is expected to limit the rates of water uptake relative to the case where only heat transport control is operating. It can be seen also that in the absence of resistance to mass transport, heat transport is sufficiently faster in air than in vacuum so that it alone would allow much higher rates of sorption. Hence any observed reduction in sorption rates in air relative to a vacuum must be a consequence of the mass transport component.

It is interesting to note that in all three cases shown in Figs. 1–4, the observed data are best described by the combined mass–heat transport model expressed by Eq. 33 when the vapor diffusion layer is assumed to be equal to the chamber dimension. Furthermore, measured ΔT values associated with sorption in air were observed to be depressed as much as 30–50% relative to values obtained at the same RH_i under an atmosphere of pure water vapor. This result is consistent with the lower ΔT value predicted for sorption controlled by both mass and heat transport.

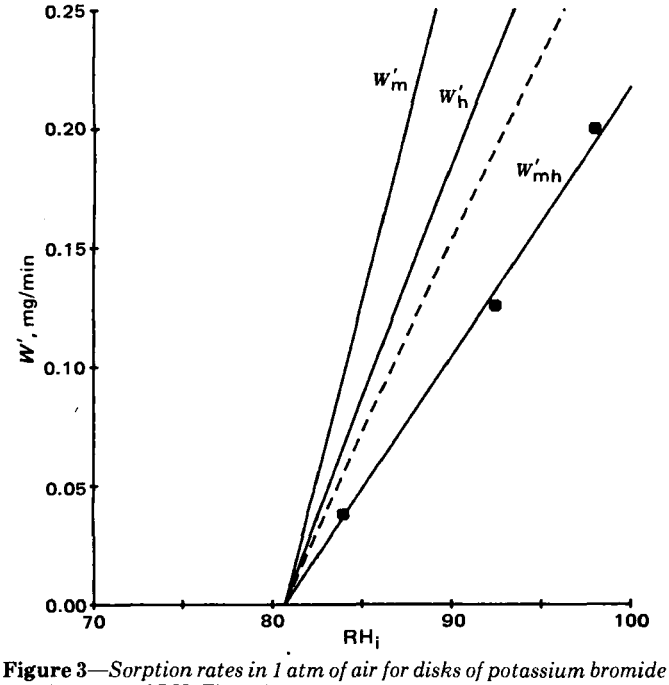

Figure 3—*Sorption rates in 1 atm of air for disks of potassium bromide as a function of RH. The solid lines are theoretical sorption curves for* W'_m, W'_h *(air), and* W'_{mh} *plotted according to Eqs. 13, 19 and 33, respectively. The dashed line presents the corresponding theoretical curve for heat transport-controlled sorption in the absence of inert gas.*

DISCUSSION

The results of studies in air, and previous work in an atmosphere of pure water vapor (1, 2), clearly indicate the importance of heat transport and mass transport as underlying mechanisms in the process of water sorption by water-soluble substances. The study of sorption in a vacuum provides a convenient approach for carrying out fundamental studies which demonstrate the importance of heat transport in these systems. Since convective flow of water vapor in the absence of an inert gas is rapid, constant pressure is immediately established throughout the chamber, making uncontrolled geometrical factors arising from equipment design relatively unimportant. In contrast, diffusional resistance to water vapor flow in air, from source to sample, retards the establishment of steady-state sorption and renders the system highly sensitive to the geometry of the sample chamber. To overcome this problem requires equipment design which emphasizes better control of vapor delivery to the solid surface. Even though our experimental results agree well with the combined heat–mass transport model, assuming minimum uptake at $\delta = b - a$, the present apparatus does not allow for flexibility in varying geometric factors.

Given the constraints of undetermined geometric factors which control mass transport of vapor, equations derived to include both heat and mass transport mechanisms are very successful in accounting for observations made when water sorption takes place in an atmosphere consisting of air and water vapor. The importance of heat transport, not previously discussed in the context of water uptake by deliquescent substances, seems

firmly established from both previous studies of sorption in the absence of air (1, 2) as well as the present study in which the moderating effects of diffusion are evident.

APPENDIX: GLOSSARY[3]

a' radius of sphere bounded by outside radius of vapor diffusion layer
c molar gas concentration; also subscript denoting "chamber"
C^* dimensionless concentration variable
k_h mass transport coefficient associated with heat transport-controlled aspect of sorption
k_m mass transport coefficient associated with mass transport-controlled aspect of sorption
P_i pressure of inert gas
P_T total pressure
P^* dimensionless pressure variable
RH_s unknown relative humidity at the sample surface associated with conditions of balanced heat and mass transport in which the two processes control sorption to a similar degree
RH^* dimensionless relative humidity variable
W_{sp} sorption rate per unit surface area
W_m sorption rate associated with mass transport control
W_{mh} sorption rate associated with the combined control of both heat and mass transport
x_w mole fraction water vapor
δ vapor diffusion layer thickness

[3] Refer to the first paper in this series (1) for the majority of symbol identification. Listed here are only those symbols introduced in the present paper.

REFERENCES

(1) L. Van Campen, G. L. Amidon, and G. Zografi, *J. Pharm. Sci.*, **72,** 1381 (1983).
(2) L. Van Campen, G. L. Amidon, and G. Zografi, *J. Pharm. Sci.*, **72,** 1388 (1983).
(3) S. Gal, "Die Methodik der Wasserdampf-Sorption-messungen," Springer-Verlag, Berlin, 1967, p. 21.
(4) M. M. Markowitz and D. A. Boryta, *J. Chem. Eng. Data*, **6,** 16 (1961).
(5) R. B. Bird, W. E. Stewart, and E. N. Lightfoot, "Transport Phenomena," Wiley, New York, N.Y., 1960, p. 505.
(6) R. C. Reid, J. M. Prausnitz, and T. K. Sherwood, "The Properties of Gases and Liquids," 3rd ed., McGraw-Hill, New York, N.Y., 1977, pp. 508–509.
(7) R. B. Bird, W. E. Stewart, and E. N. Lightfoot, "Transport Phenomena," Wiley, New York, N.Y., 1960, p. 432.

ACKNOWLEDGMENTS

Submitted by L. Van Campen to the University of Wisconsin–Madison in 1981, in partial fulfillment of the doctor of philosophy degree requirements.

L.V.C. expresses appreciation for graduate fellowship support to the American Foundation for Pharmaceutical Education and Merck Sharp and Dohme Research Laboratories.

Quantitative Determination of Benzoyl Peroxide by High-Performance Liquid Chromatography and Comparison to the Iodometric Method

NEHRU GADDIPATI ˣ, FRANK VOLPE, and G. ANTHONY

Received June 14, 1982, from the *Quality Services Department, R&D Division, Revlon Health Care Group, Tuckahoe, NY 10707.* Accepted for publication October 14, 1982.

Abstract □ A selective high-performance liquid chromatographic (HPLC) procedure for the quantitative determination of benzoyl peroxide in pharmaceutical dosage forms is described. Benzoyl peroxide was dissolved or extracted in the presence of an internal standard, acenaphthylene. The specificity of the stability-indicating HPLC and iodometric procedures are presented for benzoyl peroxide.

Keyphrases □ Benzoyl peroxide—degradation products, stability-indicating high-performance liquid chromatography, comparison with iodometric procedures □ High-performance liquid chromatography—stability indicating, benzoyl peroxide and its degradation products, commercial formulations, comparison with iodometric procedures □ Degradation products—benzoyl peroxide, stability-indicating high-performance liquid chromatography in commercial formulations.

Benzoyl peroxide (dibenzoyl peroxide), active against acne-causing bacteria, is widely used in pharmaceutical preparations as an antibacterial and keratolytic agent (1). Analytical methods currently available include spectrophotometry (2), polarography (2), TLC (3), titrimetry (4), and high-performance liquid chromatography (HPLC) (5, 6).

BACKGROUND

Benzoyl peroxide is a chemically reactive molecule which readily decomposes in various solvents (7) to give compounds such as biphenyl, phenyl benzoate, benzoic acid, benzene, 4-biphenylcarboxylic acid, homophthalic acid, homoterephthalic acid, and carbon dioxide (8). Daley *et al.* reported a selective titrimetric procedure (9), modifying the conventionally utilized iodometric method. They proposed the addition of phenyl sulfide prior to the titration to eliminate potential interferences caused by the presence of hydroperoxide impurities such as perbenzoic acid. This iodometric procedure has been accepted as the USP method for analysis of benzoyl peroxide lotion (10). Oliveri-Vigh and Hainsworth proposed an HPLC procedure that is selective in the presence of benzoic acid and benzaldehyde (5). Burton *et al.* proposed a similar HPLC procedure specific for analysis of benzoyl peroxide in gels and lotions in the presence of benzoic acid and perbenzoic acid (6); this procedure has been adopted as the USP method for analysis of benzoyl peroxide gel (11).

Analyses of benzoyl peroxide using Burton *et al.*'s procedure or the compendial HPLC procedure (6, 11) may give less accurate results, because this method depends on the use of an homogeneous reference standard. The aforementioned analytical procedures utilize aqueous benzoyl peroxide as the reference material to prepare the standard solutions. Aqueous benzoyl peroxide (70% benzoyl peroxide) is a heterogenous mixture which is nonuniform in its water content, typically varying

0022-3549/83/1200-1398$01.00/0